Biochimica et Biophysica Acta, 1016 (1990) 235–243
Elsevier

BBABIO 43196

Millisecond time-resolved EPR of the spin-polarised triplet in the isolated Photosystem II reaction centre

Geoffrey F.W. Searle [1], Alison Telfer [2], James Barber [2] and Tjeerd J. Schaafsma [1]

[1] *Department of Molecular Physics, Agricultural University, Wageningen (The Netherlands) and* [2] *Department of Biochemistry, Imperical College of Science and Technology, London (U.K.)*

(Received 24 October 1989)

Key words: Photosystem II; Reaction center; ESR; Millisecond decay kinetics; Microwave power; Triplet state

The D_1/D_2-cytochrome *b*-559 PS II reaction centre was isolated using Triton X-100, and this detergent was subsequently exchanged for dodecyl β-maltoside. This preparation is stable in the dark, and at cryogenic temperatures in the light. The isolated PS II reaction centre showed a steady-stage $\Delta m = 1$ EPR spectrum of a chlorophyll triplet state, at temperatures under 20 K. Its polarisation pattern was AEEAAE, characteristic of the molecular triplet state of the primary donor (^{3}P680) populated exclusively in the T_0 level via the ^{3}RP. Increasing the temperature within the range 5–20 K caused a decrease in EPR signal intensity (the *z* peak being initially more sensitive than the *x* or *y* peaks), but the polarisation pattern remained unchanged. The millisecond time-resolved response of the intensity of the *x*, *y* and *z* peaks to a light excitation step pulse was measured, and the light-on and -off responses could all be described by a single exponential at low (≤ 30 μW) microwave power and low (≤ 100 mW) light intensity. The values of the decay rate constants, k_x, k_y and k_z, extrapolated to zero microwave power, were compared with values reported for PS II preparations of larger antenna size. The value for k_x, 605 s^{-1}, was distinctly shorter than those previously reported, and tended towards that reported for biligated monomeric Chl *a* in methyltetrahydrofuran. k_x was found to be extremely sensitive to microwave power. The value for k_z was 185 s^{-1}, and that for k_y 965 s^{-1}. A second exponential component was seen in the kinetics of the *y* and *z* peaks at high microwave power due to a non-negligible microwave-induced population of the $T_{\pm 1}$ levels. The decay rate constants were all independent of the wavelength (458 or 514 nm) and intensity (50–300 mW) of the excitation light. They remained unchanged when the steady-state EPR signal intensity was reduced by 50% by increasing the temperature. This was taken to indicate that the effect of temperature was on the populating process. A theoretical model has been developed which can explain most of the effects of microwave power on the EPR kinetics.

Introduction

The Photosystem II (PS II) reaction centre (RC) can be isolated in a purified form containing only about 4–5 chlorophyll (Chl) *a* per cytochrome *b*-559, bound to a D_1/D_2 polypeptide heterodimer [1,2]. This preparation does not evolve O_2, but still has a secondary donor, probably Z [3,4]. On the acceptor side there are two pheophytins, but no quinones corresponding to Q_A and Q_B. Whether the non-haem iron is present in its native state is uncertain [4,5].

The availability of the D_1/D_2 preparation represents an important step forward in studies of the primary processes in PS II. Its usefulness, however, depends critically on the integrity of the RC compared to that in intact chloroplasts. It is possible that the primary electron donor, P680, which is attached to the D_1/D_2 heterodimer and is believed to be either a monomer or a dimer of Chl *a*, could be altered in structure due to the loss of these components from the PS II RC.

In order to further test the integrity of P680 in D_1/D_2 we have investigated the properties of its spin-polarised molecular triplet state (^{3}P680). This state is populated from the triplet radical pair (^{3}RP), which is generated in the RC by primary electron transfer from P680 to one of the pheophytins, followed by a spin-dephasing process. In high magnetic field the three levels of the ^{3}RP are split and only its T_0 level can be populated via the ^{1}RP. This characteristic population

Abbreviations: PS II, Photosystem II; Chl, chlorophyll; RP, radical pair; RC, reaction centre; EPR, electron paramagnetic resonance; SLR, spin lattice relaxation, T_0, triplet spin state $m_s = 0$.

Correspondence: G.F.W. Searle, Department of Molecular Physics, Agricultural University, 6703 HA Wageningen, The Netherlands.

distribution over the three levels gives rise to the polarised triplet state in the high magnetic fields used in EPR experiments [6]. ^{3}P680 can be generated in D_1/D_2 in high yield at cryogenic temperatures [5,7], and therefore can be used as an internal probe of the RC structure, because the decay rates to the ground state of the three triplet spin levels $|x>$, $|y>$ and $|z>$, which can be measured by millisecond time-resolved EPR, are sensitive to changes in the P680 microenvironment [8].

The decay rate constants of the three triplet spin levels have already been reported for PS II preparations still containing a high proportion of antenna chlorophyll, using both EPR [9] and absorption detected magnetic resonance [10] techniques. Flash-induced absorption transients, which were attributed to ^{3}P680, gave a mean molecular decay rate constant of 770 s^{-1}, which was independent of temperature between 5 and 120 K [11]. It should be emphasised that, in contrast to EPR, the individual triplet spin levels cannot be distinguished using absorption techniques. These preparations would be expected to be less susceptible than D_1/D_2 to structural changes of the RC, compared to the PS II RC in intact chloroplasts. Comparison of triplet state decay rate constants for D_1/D_2 with that for the other types of PS II preparation should therefore give information on any possible changes which might have taken place in the D_1/D_2 RC structure during its isolation.

In addition, time-resolved EPR studies on the isolated RC can have other implications. The temperature dependence of the EPR spectrum of the primary donor triplet state in the *Rhodopseudomonas viridis* RC has been previously reported, and a characteristic sign inversion of the *y* peak above 20 K was observed [12]. This was explained by a change in the kinetics of the *y* peak with temperature, which was in turn attributed to an anisotropic relaxation process due to transfer of the Fe^{2+} spin-lattice relaxation (SLR) via the singly reduced menaquinone, Q_A^-, to the reduced primary acceptor, I^- [13]. As D_1/D_2 lacks the quinones Q_A and Q_B it would not be expected that a similar sign inversion would be observed in this PS II RC preparation, whether or not the non-haem iron is still present, and this has been recently confirmed [14]. However, there is a possibility that reconstitution studies could be carried out successfully on D_1/D_2 in the near future [15]. EPR kinetics, and the sign of the peaks in the EPR spectrum as a function of temperature, would then be useful parameters to monitor the reconstitution. The experiments reported in this paper are therefore also an initial investigation of the EPR kinetics of the current quinone/iron-less preparation with future reconstitution studies in mind.

An interesting and significant difference between PS II and the purple photosynthetic bacterial RC has recently been reported. It has been shown that ^{3}P680 is generated only in RC's in BBY particles (a PS I preparation with a large antenna size) from which Q_A has been lost [16]. Therefore in these particles the interactions of Q_A^- with other paramagnetic species cannot be measured through the EPR spectrum and kinetics of ^{3}P680. Whether the same situation holds for D_1/D_2 remains to be determined.

Materials and Methods

Materials

The PS II reaction centre was isolated essentially as described by Chapman et al. [17]. In the initial experiments the samples contained Triton X-100, but in later measurements dodecyl β-maltoside replaced the Triton X-100. No difference in EPR kinetics was observed between the two preparations. The samples were diluted with 50 mM Tris-HCl (pH 8.0) to a concentration of 80 μg Chl/ml and a final concentration of 0.07% Triton X-100 or 0.8 mM dodecyl β-maltoside. Although not strictly required, 10 mg/ml sodium dithionite was added routinely, as this was found to increase the size of the triplet EPR signal. After dark adaptation, the samples were cooled rapidly in complete darkness to 77 K before carrying out the measurements at liquid helium temperatures.

EPR kinetics

The Varian E-6 EPR spectrometer was equipped with a helium flow cryostat and ITC-4 temperature control system (Oxford Instruments). The light step pulses (10 ms light, followed by 20 ms dark) had a rise time no greater than the dwell time of the signal sampling system (typically 20 μs), achieved by focusing the continuous wave Ar-ion laser beam (458 or 514 nm) in the plane of a mechanical chopper. The averaged signal from 30 000–60 000 sweeps was stored in a computer of average transients (EG&G 4203), triggered by means of a photodiode at the light-on or light-off flank. The kinetic traces were fitted to a sum of 1–2 exponentials using the programme SPLMOD (R. Vogel, EMBL Heidelberg) on a VAX computer.

Results

Steady-state EPR

The samples were first characterised using steady-state EPR. Fig. 1 shows spectra obtained in a single sweep at two temperatures (only the low field region is shown). The polarisation pattern was AEEAAE. The triplet spin levels are labelled *x*, *y* and *z*, in decreasing order of energy. At 10 K the amplitudes of the signal at the *x*, *y* and *z* peaks has decreased by about 50% compared to that at 5 K. Within the experimental error the spectrum remained symmetrical and there was no sign reversal of any of the peaks over the range 5–20 K.

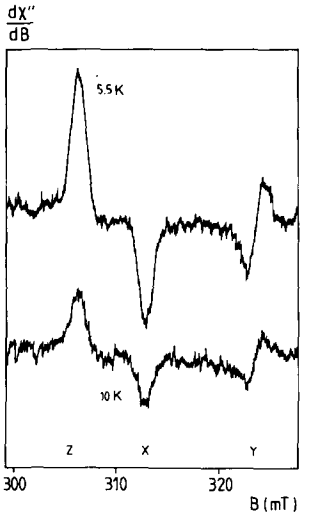

Fig. 1. Steady-state EPR spectrum of D_1/D_2. Only the low-field part of the spectrum is shown, as the spectrum is symmetrical within the experimental error. Gain, $2 \cdot 10^4$; modulation amplitude, 2 mT; 9.225 GHz. Light intensity, 200 mW. Temperature, 5.5 K (upper), 10 K (lower).

in agreement with the findings of Frank et al. [14]. The triplet state is characterised by the zero-field-splitting parameters $D = 0.0283$ cm^{-1} and $E = 0.0041$ cm^{-1}.

EPR kinetics

Typical responses of the EPR signal to the light step pulse (light on at zero time, light off at downward arrow) are shown for the x, y and z peaks in Fig. 2. At high light intensity (200 mW) and high microwave power (≥ 100 μW, Fig. 2A) the response to light-on and light-off was biphasic for y and z, but a single exponential adequately described the kinetics at low light intensity (100 mW) and low microwave power (Fig. 2B). The biphasic character of the x peak during the light-on period, shown in Fig. 2A, was seen at high (> 100 mW) light intensity only, and the x peak light-on response was monoexponential at high microwave power and low light intensity (not shown).

Fig. 3 shows that the rate constants were all found to be dependent on microwave power. The dependence was non-linear, as expected from the theoretical treatment (see Appendix Eqns. 12,13). These measurements were carried out at low light intensity (< 100 mW). The light-on and light-off responses are identical within experimental error, indicating the absence of trigger jitter artefacts. Note that the x peak kinetics are particularly sensitive to microwave power, the rate constant increasing 4-fold over the range 0.01 to 0.3 mW. In contrast, the kinetics of the z are little changed over the same range. It is interesting to note the difference between our results and those of Gast and Hoff [18], who found that the z-peak kinetics were the most sensitive to microwave power in a photosynthetic bacterium. The decay rate constants obtained at the

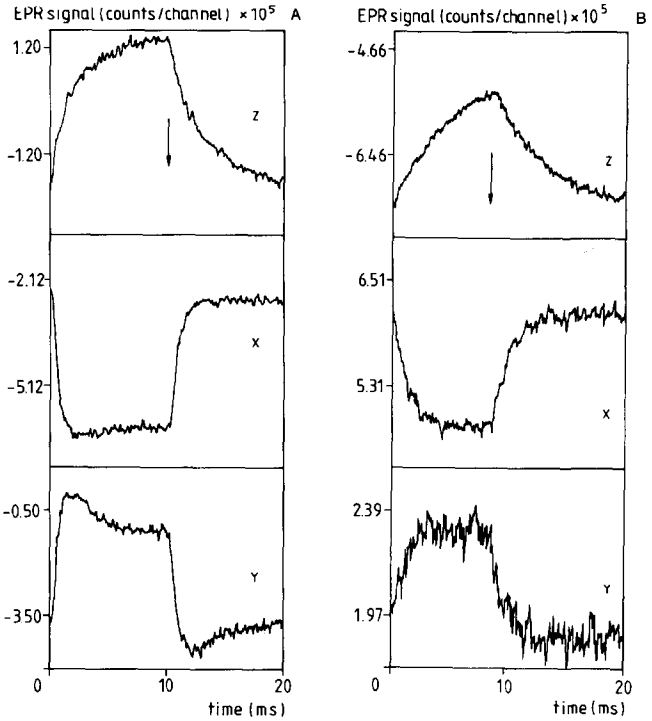

Fig. 2. Time-resolved response of the x, y and z peaks in the EPR spectrum to a light step pulse at (A) 100 μW, and (B) 10 (y) and 30 (x,z) μW microwave power. The response at 10 μW is shown for the y peak because a residual biphasicity could still be seen for this peak at 30 μW. At 10 μW the response of the x and z peaks were essentially the same as those shown for 30 μW but with a lower signal/noise ratio. Note that the variation in the signal sizes in A and B can be directly compared. The absolute signal sizes contain an arbitrary back-off level, which is different for each of the kinetic traces shown. Temperature, 5.5 K. Light intensity: (A) 200 mW, showing the effect of high light intensity on the x peak kinetics; (B) 100 mW, to avoid light-induced biphasicity of the kinetics.

lowest microwave power, 10 μW, are collected in Table I, and compared with literature values for other PS II preparations and Chl *a*.

TABLE I

Decay rate constants (s^{-1}) for the x, y and z peaks in the EPR spectrum of PS II and Chl a

Temperature ≈ 5 K.

Source	z	x	y
PS II [a]	110± 5	930± 40	1088± 50
PS II [b]	165	990	690
D_1/D_2 [c]	185±20	605± 60	965±100
Chl *a*·MTHF [d]	180±30	1180±120	830± 80
Chl *a*·2MTHF [e]	150±25	310± 40	930± 90

[a] Den Blanken et al. [10].

[b] Rutherford et al. [9], error margins not quoted.

[c] This report, 10 μW microwave power (see Fig. 3), error margin ±10%.

[d,e] Mono- and biligated Chl *a* in methyltetrahydrofuran (MTHF) at 4.2 K [21].

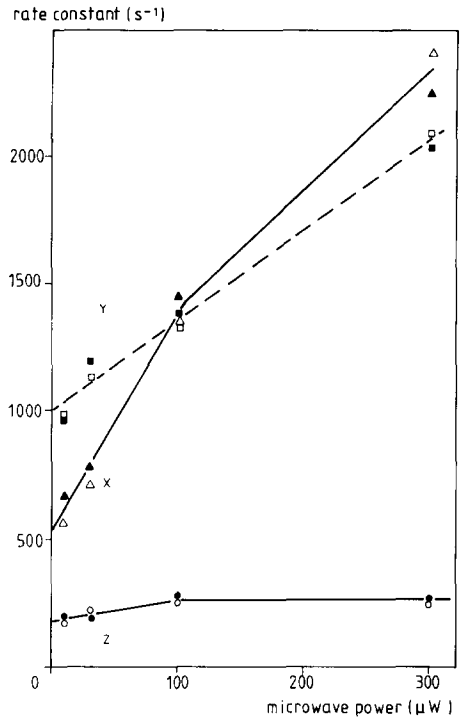

Fig. 3. The dependence of the measured rate constants for the x, y and z peaks on microwave power. Light excitation intensity 95 mW, wavelength 514 nm. The temperature was 5.3 K. Closed symbols show the light-on response, and open symbols the light-off response. The experimental error is typically ±5%.

Fig. 4 shows that the rate constants were all found to be independent of the light excitation intensity, over the range 50–300 mW, within the experimental error (error bars shown). The values for 65, 165 and 300 mW were obtained using 458 nm light, the others with 514 nm. The values shown are averages of several light-on and light-off responses. Only the data for the slower exponential component for z, and the faster component for x and y (see Fig. 2A) are presented, as these should represent the rate constant for decay out of the T_0 level (see Discussion and Appendix). The faster component in the z peak, and the slower component in the y peak should reflect decay out of the $T_{\pm 1}$ levels, populated because of the high microwave-induced transition rate from T_0 (see Discussion and Appendix). Fig. 4 also shows the decay rate constants did not change on raising the temperature from 5.5 K to 10 K, although there was a concomitant 2-fold decrease in EPR signal intensity (Fig. 1).

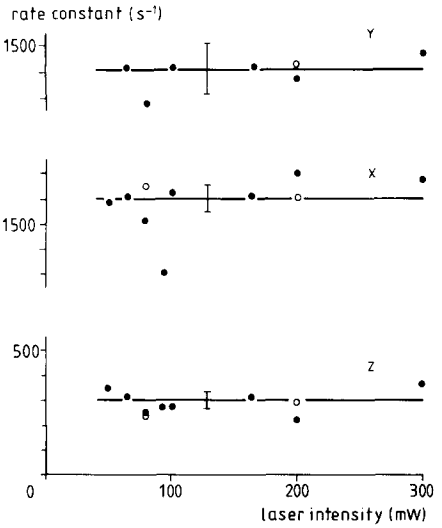

Fig. 4. The dependence of the measured rate constants for the x, y and z peaks on light intensity and also on temperature. Temperature 5.5 K, except for the data points marked with open circles: 10 K. Microwave power was 100 μW.

Discussion

The isolated D_1/D_2 PS II RC preparation shows a spin-polarised triplet EPR spectrum with polarisation AEEAAE (Fig. 1), which we attribute to the molecular triplet state of the RC primary donor, formed as shown in Fig. 5. The speculation of Rutherford [19] that the triplet state resides instead on an accessory Chl a in close contact with the primary donor has not yet been confirmed. However, in either case the observed triplet state can be a useful probe of the microenvironment of the RC, on the assumption that the same triplet state has been studied both here in D_1/D_2 and in the PS II preparations with larger antenna size [9,10].

The intensity of the spectrum increased after addition of dithionite, which presumably ensured that $P680^+$ was completely reduced before low-temperature illumination. The intensity had a microwave power optimum at 100 μW at 5 K, although at this power level the kinetics were already biphasic indicating a partial population of the $T_{\pm 1}$ levels (see Appendix). It did not show light saturation even at 300 mW excitation intensity.

In the experiments to measure the EPR kinetics of D_1/D_2, using the method described in Materials and Methods, consideration has to be given to processes which might complicate interpretation of the results:

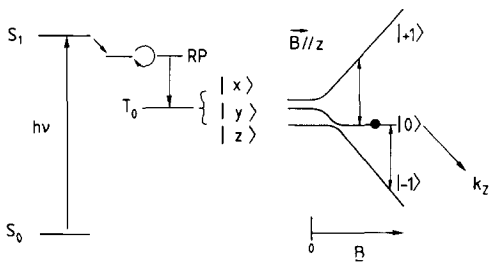

Fig. 5. The primary processes which lead to the P680 molecular triplet state via charge separation and recombination in PS II, and the origin of the high-field EPR peaks. The three spin levels are split in the high EPR magnetic field (B) into the $|+1>$, $|0>$ and $|-1>$ states. Only the population of the $|0>$ state is non-zero, This is illustrated for the z-peaks (magnetic field parallel to the molecular z-axis). RP: triplet radical pair.

(1) Excitation light intensity. High intensities might speed up the measured decay kinetics through triplet-triplet (T-T) absorption. T-T absorption would also be dependent on the excitation wavelength.
(2) SLR, caused by interaction of ^{3}P680 with vibrational states of the surrounding protein, would also speed up the measured decay kinetics. SLR would be temperature-dependent.
(3) Microwave power. High power levels have been shown to cause a speeding up of the measured triplet state decay kinetics in a photosynthetic bacterium; however, this effect was negligible at levels no greater than 20 μW [18].

In principle, if we perform the measurements of the EPR kinetics at low excitation light intensity, at low temperature, and at low microwave power, then we can expect to obtain the true triplet state decay rate constants for the individual x, y and z peaks.

As clearly seen in Fig. 4, increasing the light excitation from 50 to 300 mW (incident on the frozen, scattering sample) in our light step pulse experiments did not cause an increase in the measured decay rate constants. This is similar to the results of Gast and Hoff [18], who found that the EPR kinetics of the triplet state of the primary donor in a photosynthetic bacterium was independent of the intensity of the laser flash excitation. This contrasts, however, with the strong dependence on light intensity of triplet state decay rate constants measured indirectly via fluorescence techniques [8].

Gast and Hoff [18] could model their results by assuming an SLR rate of 500 s^{-1}. SLR cannot be so fast in D_1/D_2 at about 5 K, however, as we have shown that the measured rate constants are unchanged on raising the temperature to 10 K (Fig. 4). Furthermore, the decay kinetics are monoexponential if low microwave power is used (Fig. 2). There is also further qualitative evidence against a significant SLR in this temperature range. SLR (within the ^{3}RP) would have caused partial population of the $T_{\pm 1}$ levels, with the population in T_{-1} being larger than that in T_{+1}, giving in turn an assymetry to the EPR spectrum [20]. However, the steady-state EPR spectrum remained symmetrical, within the experimental error, up to 20 K.

There remains the effect of microwave power on the kinetics and, as is shown in Fig. 3, the decay rate constants are indeed strongly dependent on the power level. It is essential therefore to use the values of the decay rate constants found at low (≤ 20 μW) microwave power in our comparisons with previously reported values.

The decay rate constants found for D_1/D_2 are compared in Table I with those reported for PS II RC preparations having a larger antenna size [9,10] and also with values for Chl a in methyltetrahydrofuran, measured with EPR at liquid helium temperature [21]. In all cases the customary notation for the labelling of the triplet spin levels, in decreasing order of energy $x > y > z$ (see for example Ref. 21) was used. Ligation to the Mg atom of Chl a in vitro has large effects on the decay rate constants of the triplet spin levels (for a review see Ref. 8). These in vitro values are suitable for purposes of comparison with PS II, because Chl a in the PS II Chl-proteins may be either mono- or biligated, most likely to either O or N atoms of the polypeptide. In principle we would expect that values for the PS II preparations would be comparable; however, this is not found to be so. Unless previously reported values are distorted by artefacts, there are apparently some differences between D_1/D_2 and the other PS II preparations. The D_1/D_2 particle is interesting for biophysical measurements because it is a highly purified RC preparation, lacking the CP29, CP43 and CP47 antenna Chl-proteins. However, the RC is apparently rather open to the external medium, as components are lost from the acceptor complex [5]. This makes it a suitable subject for reconstitution studies, but also brings into question the intactness of the RC in the isolated D_1/D_2.

The value of the rate constant for the y peak (k_y) is very similar to that found by Den Blanken et al. [10], and also to those for monomeric Chl a ligated to methyltetrahydrofuran [21]. The approximate value of k_y quoted by Rutherford et al. [9] is distinctly smaller, which could be a result of incomplete resolution within the noise of the two components of opposite sign in the y-peak kinetics (Fig. 2A).

The value of the rate constant for the z peak (k_z) in D_1/D_2 is larger than that reported previously for a PS II RC preparation with a larger antenna size [10]. This could indicate a slight disturbance in the ligation of the Chl a in P680 in D_1/D_2, but a definite conclusion should await a more comprehensive investigation of the other types of PS II preparation.

The kinetics of the x peak are the most variable amongst the reported measurements, and there seems to be a clear difference between the values for D_1/D_2, and for the other PS II preparations (Table I). The values of k_x for Chl a is seen to be extremely sensitive to ligation by methyltetrahydrofuran (Table I). Previously reported values for PS II preparations are in reasonable agreement with the value for monoligated Chl a. The value for D_1/D_2, however, clearly lies between the values for mono- and biligated Chl a. This is strong evidence for a perturbation of P680 in the isolated PS II RC, the exact nature of which remains to be determined.

When light is turned on or off the population of the T_0 level changes at a rate primarily determined by its decay rate constant, k_0. The EPR spectrum intensity is proportional to the difference in population of the coupled T_0 and $T_{\pm 1}$ levels, so that if a high microwave power is applied and the transfer of molecules from the T_0 to the $T_{\pm 1}$ levels becomes significant, then this causes a reduction in the EPR signal size. The effect of

TABLE II

Measured and calculated kinetic rate constants (s^{-1}) for the x, y and z peaks of the EPR spectrum of D_1/D_2

See text for details.

Rate constant	z	x	y
k_0	185	605	965
k_1	785	575	395
$\|k_1 - k_0\|$	600	30	570
$(k_0 + k_1)/2$	485	590	680

microwave power on the measured EPR kinetics is two-fold: not only is there an apparent increase in the decay rate constant out of T_0 as seen in Fig. 3, but there is also the induction of a second component, which produces the biphasic kinetics shown in Fig. 2A. This second component is seen most clearly in the EPR kinetics of the y and z peaks at high microwave power and is a consequence of a non-zero population of the $T_{\pm 1}$ levels (see Appendix). In the case of the z peak this component has a much faster rate constant $(k_x + k_y)/2$ than that of the first component, k_z, and an amplitude with the same sign as the first component i.e. both absorptive. In the case of the y peak, the second component has a much smaller rate constant $(k_x + k_z)/2$ compared to the first component, k_y, and an amplitude of opposite sign, i.e. absorptive instead of emissive. The origin of the difference in sign of the second component compared to that of the first lies in the different values for k_0 and k_1 for the x, y, and z peaks (see Eqns. 20 and 21 in the Appendix). The x peak apparently does not show a second component induced by high microwave power. This is simply due to the difficulty in resolving two components with very similar rate constants: k_x and $(k_y + k_z)/2$ (see the values in Table I).

The rate constants, which according to the theory outlined in the Appendix determine the kinetics of the x, y and z peaks, are presented in Table II. The values of k_0 are taken from Table I assuming that k_0 is equal to the decay rate constant measured at 10 μW, and k_1 is calculated from $k_{1,i} = (k_{0,j} + k_{0,k})/2$ (see Fig. 6). From Eqns. 26,27 we see that the variation of the two roots, λ_1 and λ_2, with microwave power is determined by $(k_1 - k_0)/2\omega$, where ω is related to the microwave power. If $|k_1 - k_0|$ is small, as is the case for the x peak

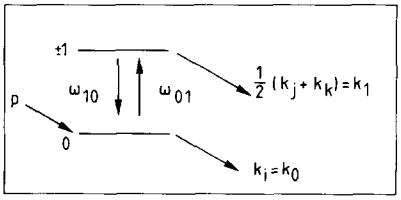

Fig. 6. The kinetic system of two levels coupled by a microwave field in EPR.

(see Table II), then a microwave-induced increase in the measured decay rate constant will be found already at low power levels. In contrast, k_z should show little variation in this microwave power range, as $|k_1 - k_0|$ is large. These effects are indeed seen in Fig. 3; however, the variation of k_y in Fig. 3 is larger than would be predicted from the theory. The other set of values shown in Table II are those of $(k_0 + k_1)/2$, which represents the limit to which λ_1 will tend at high microwave power (see Appendix).

The rate constant of the second kinetic component was for the z peak, 1617 s^{-1} at 300 μW, and 1277 s^{-1} at 100 μW, linearly extrapolating to 1107 s^{-1} at zero power; and for the y peak, 495 s^{-1} at 300 μW, and 449 s^{-1} at 100 μW, linearly extrapolating to 427 s^{-1} at zero power (for all values, the experimental error was 10–20%). The theory predicts that the values at zero microwave power should correspond with the values of k_1 in Table II, and it is seen that there is indeed reasonable agreement.

From the experimentally observed microwave power dependency of the rate constants (Fig. 3) it would appear that the slow component in the z peak kinetics, which dominates at low microwave power, corresponds to λ_1 as expected, and the faster second component to λ_2. For the x peak, although at low microwave power we may be measuring λ_1, we must in fact assume that we observe λ_2 at higher powers in order to explain the measured strong power dependence (Fig. 3), because λ_1 is practically independent of microwave power (605 → 590 s^{-1}, Table II). For the y peak several discrepancies of theory and experiment are apparent. The large value of $|k_1 - k_0|$ in Table II corresponds better with the weak microwave dependence of the slow component (see above), than with the pronounced dependence of the faster component (Fig. 3). The predicted decrease in λ_1, going from 965 to 680 s^{-1} as the microwave power increases (Table II), does not agree with the experimental findings, and moreover the theory predicts that $-\lambda_1(k_0) \leq -\lambda_2(k_1)$. It would appear therefore that at non-zero microwave power the slower component (± 400 s^{-1}) corresponds better with λ_1 and that the faster component (965 s^{-1}) corresponds better with λ_2. Therefore, for the y peak the agreement of the theory with the experimental data is not complete, indicating that either the theory requires further refinement or that the experimental measurements are being complicated by, for example, the overlap of the peaks in the EPR spectrum.

Raising the temperature to 10 K did not change the values for the decay rate constants (Fig. 4), whereas the steady-state spectrum decreased more than two-fold in intensity (Fig. 1). We do not present a detailed analysis of the dependence on temperature, as we only wish to emphasise that a change in EPR signal intensity can occur without a significant change in the measured

decay rate constants. The reported invariance of the average of the decay rate constants for the three spin levels, measured by absorption transients over the temperature range 5–120 K [11], is in line with our result. Note that the EPR signal, in contrast to the absorption transients, is already lost at 20 K. At temperatures above 10 K the EPR signal was too small to obtain kinetic data with sufficient signal/noise ratio under our experimental conditions.

A decrease in EPR intensity with increasing temperature could be due to a 2-fold decline in the triplet quantum yield; however, evidence against this possibility is that the intensity of the z peak did not decrease in parallel with the x and y peaks within the range 5–10 K (not shown). This effect has also been observed in a PS II sample prepared according to the procedure of Ghanotakis et al. [22] (Van Mieghem, F.J.E. and Searle, G.F.W., unpublished observations). The decrease in the EPR spectrum intensity is therefore probably due to a decrease in the difference in population of the T_0 and the $T_{\pm 1}$ levels, caused by a non-zero population of the $T_{\pm 1}$ levels. At low microwave power the microwave-induced transition rate from T_0 to $T_{\pm 1}$ is negligible. Also, as discussed above, SLR can be neglected in our experiments at 5 K. The remaining possibility for population of $T_{\pm 1}$ is that the effect of temperature is on the population rates of the molecular triplet state. We tentatively suggest that, on increasing the temperature, the exclusive population of the T_0 level no longer holds, because of a temperature-induced perturbation, which causes a transfer of population within the triplet radical pair, which in turn leads to a non-zero population of the $T_{\pm 1}$ levels of the molecular triplet.

Fig. 2 shows that high light excitation intensity induced a second component specifically in the light-on, and not in the light-off, kinetics of the x peak. Although we cannot present a complete explanation for this effect, it is possible that it is also due to a relaxation process between the T_0 and $T_{\pm 1}$ levels, caused by an anisotropic interaction with a light-induced paramagnetic species along the triplet x axis. This effect of high excitation intensity may therefore be related to the significant decrease in k_x in D_1/D_2 compared to the other PS II preparations (Table I).

Acknowledgements

We wish to thank Professor A.J. Hoff for discussions on the effect of microwave power on EPR kinetics. Adrie de Jager and Arie van Hoek gave invaluable assistance with the EPR and cryogenic apparatus, respectively. Frans van Mieghem is thanked for the measurements on the temperature-dependence of the EPR spectrum of the PS II particles. This work was supported by a Wageningen Agricultural University fellowship to A.T.

Appendix

The EPR spectrum size will naturally depend on the microwave power: the higher the power, the better the S/N ratio. However, if the power is too high, then the populations of the two levels coupled by the microwave field will tend to be equalised and the EPR spectrum decreases (saturation). At the same time, the rate constants describing the response to a light block pulse will be increased by the cycling between the levels, which is induced by the microwave field.

In Fig. 6 the T_0 level is populated selectively from the ^{3}RP T_0 level during the light-on period, due to conservation of the spatial quantisation of the triplet spin during the radiationless transition from ^{3}RP to ^{3}P680. We will assume that $\omega_{10} = \omega_{01} = \omega$. We can write:

$$dn_0/dt = -(\omega + k_0)n_0 + \omega n_1 + p \quad (1)$$

$$dn_1/dt = +\omega n_0 - (\omega + k_1)n_1 \quad (2)$$

In the steady-state situation:

$$dn_0/dt = dn_1/dt = 0 \quad (3)$$

From Eqns. 1,2,3 we can derive:

$$n_0^{ss} = p(\omega + k_1)/\{(k_0 + k_1)\omega + k_0k_1\} \quad (4)$$

$$n_1^{ss} = p\omega/\{(k_0 + k_1)\omega + k_0k_1\} \quad (5)$$

For small ω (low microwave power) $n_0^{ss} \approx p/k_0$ and $n_1^{ss} \approx p\omega/k_0k_1$. For large ω we find that $n_0^{ss} \approx n_1^{ss} \approx p/(k_0 + k_1)$, so that the EPR signal (proportional to $n_0 - n_1$) ≈ 0, i.e., it becomes saturated as expected.

When the light is now turned off at $t = 0$, then $p = 0$, and $n_0^{ss}(n_0^0)$ and $n_1^{ss}(n_1^0)$ decay to zero. We can now write:

$$dn_0/dt = -(\omega + k_0)n_0 + \omega n_1 \quad (6)$$

$$dn_1/dt = +\omega n_0 - (\omega + k_1)n_1 \quad (7)$$

Laplace transformation and use of $L(dX/dt) = sL(X) - X_0$ gives:

$$L(n_0) = \{n_0^0(s + \omega + k_1) + \omega n_1^0\} / \{(s + \omega + k_0)(s + \omega + k_1) - \omega^2\} \quad (8)$$

and

$$L(n_1) = \{n_1^0(s + \omega + k_0) + \omega n_0^0\} / \{(s + \omega + k_0)(s + \omega + k_1) - \omega^2\} \quad (9)$$

Inverse Laplace transformation gives us expressions for the roots and the coefficients of the two exponential components, which fully describe the decay of n_0 and

n_1 after $t = 0$. Expressing the denominator in Eqns. 8,9 as $(s-\lambda_1)(s-\lambda_2)$ gives us expressions for the roots $\lambda_{1,2}$:

$$\lambda_1 + \lambda_2 = -(2\omega + k_0 + k_1) \tag{10}$$

$$\lambda_1\lambda_2 = (\omega + k_0)(\omega + k_1) - \omega_2 \tag{11}$$

From Eqns. 10,11 we derive

$$\lambda_1 = 0.5\left\{-(2\omega + k_0 + k_1) + \sqrt{[(k_1 - k_0)^2 + 4\omega^2]}\right\} \tag{12}$$

and

$$\lambda_2 = 0.5\left\{-(2\omega + k_0 + k_1) - \sqrt{[(k_1 - k_0)^2 + 4\omega^2]}\right\} \tag{13}$$

We note that if ω is small, then $\lambda_1 \approx -k_0$ and $\lambda_2 \approx -k_1$ so that λ_1 represents the expected decay rate constant of the T_0 level. The decay of n_0 is given by:

$$n_0(t) = c_1 \exp \lambda_1 t + c_2 \exp \lambda_2 t \tag{14}$$

and from the numerator of Eqn. 8 we see that

$$c_1 = \{n_0^0(\lambda_1 + \omega + k_1) + \omega n_1^0\}/(\lambda_1 - \lambda_2) \tag{15}$$

and that

$$c_2 = \{n_0^0(\lambda_2 + \omega + k_1) + \omega n_1^0\}/(\lambda_2 - \lambda_1) \tag{16}$$

In a similar way the decay of n_1 is given by:

$$n_1(t) = c_3 \exp \lambda_1 t + c_4 \exp \lambda_2 t \tag{17}$$

and from the numerator of Eqn. 9 we see that

$$c_3 = \{n_1^0(\lambda_1 + \omega + k_0) + \omega n_0^0\}/(\lambda_1 - \lambda_2) \tag{18}$$

and that

$$c_4 = \{n_1^0(\lambda_2 + \omega + k_0) + \omega n_0^0\}/(\lambda_2 - \lambda_1) \tag{19}$$

We can now inspect the value of $n_0 - n_1$, which determines the EPR signal size, for each of the two exponential components. For λ_1 this is given by $c_1 - c_3$, and from Eqns. 15,18 we see that:

$$c_1 - c_3 = \{(n_0^0 k_1 - n_1^0 k_0) + \lambda_1(n_0^0 - n_1^0)\}/(\lambda_1 - \lambda_2) \tag{20}$$

For λ_2 this is given by $c_2 - c_4$, and from Eqns. 16,19 we see that:

$$c_2 - c_4 = \{(n_0^0 k_1 - n_1^0 k_0) + \lambda_2(n_0^0 - n_1^0)\}/(\lambda_2 - \lambda_1) \tag{21}$$

We note that, because the denominators of Eqns. 20 and 21 have opposite signs, we would in general expect the two components in the time response of the EPR signal to have opposite signs, i.e., one 'absorptive' and the other 'emissive', unless the numerators in Eqns 20,21 have different signs. These numerators can in fact have opposite signs depending on whether we are measuring $|x>$, $|y>$ or $|z>$, because they are equal to the difference between a positive and a negative expression, and which is greater will depend on the values of k_0 and k_1, which of course vary for $|x>$, $|y>$ and $|z>$: $n_0^0 k_1 - n_1^0 k_0$ is always positive for small ω because from Eqns. 4,5:

$$n_0^0 k_1 - n_1^0 k_0 = \{p(\omega + k_1)k_1 - p\omega k_0\}/\{(k_0 + k_1)\omega + k_0 k_1\} \tag{22}$$

and $\lambda_{1,2}(n_0^0 - n_1^0)$ must be negative, because $n_0^0 > n_1^0$, and $\lambda_{1,2} < 0$.

To summarise:

$$S = A\{[\{(n_0^0 k_1 - n_1^0 k_0) + \lambda_1(n_0^0 - n_1^0)\}/(\lambda_1 - \lambda_2)] \exp \lambda_1 t\} + A\{[\{(n_0^0 k_1 - n_1^0 k_0) + \lambda_2(n_0^0 - n_1^0)\}/(\lambda_2 - \lambda_1)] \exp \lambda_2 t\} \tag{23}$$

where S, the EPR signal size, is positive if the transition is 'absorptive'. A, is an instrumental constant, positive if $E_1 > E_0$, and negative if $E_0 > E_1$. n_0^0 and n_1^0 are defined in Eqns. 4,5 above. k_0 is the decay rate constant of the T_0 level, and k_1 is the average decay rate constant of the levels $T_{\pm 1}$ (Fig. 6). p is the population rate constant of T_0 in the light-on period. ω is the microwave-induced transition rate constant between the level T_0 and $T_{\pm 1}$. The roots $\lambda_{1,2}$ are defined in Eqns. 12,13 above. Note that if ω is small $\lambda_1 \approx -k_0$, and $\lambda_2 \approx -k_1$; also $c_1 - c_3 \approx n_0^0$, $c_2 - c_4 \approx -n_1^0$. Therefore from Eqn. 23:

$$S = A\{n_0^0 \exp(-k_0 t) - n_1^0 \exp(-k_1 t)\} \tag{24}$$

From Eqn. 5 we see that for small ω, $n_1^0 \approx p\omega/k_0 k_1$, so that n_1^0 is negligible. Therefore:

$$S = A\{n_0^0 \exp(-k_0 t)\} \tag{25}$$

which is a monoexponential decay.

The roots given by the expressions in Eqns. 12,13 will be non-linearly dependent on the microwave power, as ω is related to the microwave power, and Eqns. 12,13 are non-linear functions of ω. We can derive the following:

$$d\lambda_1/d\omega = -1 + \{1 + [(k_1 - k_0)/2\omega]^2\}^{-1/2} \tag{26}$$

$$d\lambda_2/d\omega = -1 - \{1 + [(k_1 - k_0)/2\omega]^2\}^{-1/2} \tag{27}$$

Eqns. 26, 27 show that both roots will decrease (i.e.,

have larger negative values) as ω is increased w.r.t. $|k_1 - k_0|$. At small values of ω the slopes are -1, independent of k_1 and k_0. As ω increases from zero, λ_1, starting at $-k_0$, will tend to reach a limit, which is a minimum given by $-(k_0 + k_1)/2$. On the other hand, λ_2, starting at $-k_1$, becomes rapidly more negative without reaching a limit.

References

1 Nanba, O. and Satoh, K. (1987) Proc. Natl. Acad. Sci. USA 84, 109–112.
2 Barber, J., Chapman, D.J. and Telfer, A. (1987) FEBS Lett. 220, 67–73.
3 Mathis, P., Satoh, K. and Hansson, O. (1989) FEBS Lett. 251, 241–244.
4 Nugent, J.F.A., Telfer, A., Demetriou, C. and Barber, J. (1989) FEBS Lett. 255, 53–58.
5 Telfer, A., Barber, J. and Evans M.C.W. (1988) FEBS Lett. 232, 209–213.
6 Thurnauer, M.C., Katz, J.J. and Norris, J.R. (1975) Proc. Natl. Acad. Sci. USA 72, 3270–3274.
7 Okamura, M.Y., Satoh, K., Isaacson, R.A. and Feher, G. (1987) in Progress in Photosynthesis Research (Biggins, J., ed.), Vol. 1, pp. 379–381, Martinus Nijhoff, Dordrecht.
8 Schaafsma, T.J. (1982) in Triplet State ODMR Spectroscopy (Clarke, R.H., ed.), pp. 291–365, Wiley, New York.
9 Rutherford, A.W., Satoh, K. and Mathis, P. (1983) Biophys. J. 41, 40A.
10 Den Blanken, H.J., Hoff, A.J., Jongenelis, A.P.J.M. and Diner, B.A. (1983) FEBS Lett. 157, 21–27.
11 Takahashi, Y., Hansson, O., Mathis, P. and Satoh, K. (1987) Biochim. Biophys. Acta 893, 49–59.
12 Van Wijk, F.G.H., Gast, P. and Schaafsma, T.J. (1986) Photobiochem. Photobiophys. 11, 95–100.
13 Hore, P.J., Hunter, D.A., Van Wijk, F.G.H., Schaafsma, T.J. and Hoff, A.J. (1988) Biochim. Biophys. Acta 936, 249–258.
14 Frank, H.A., Hansson, O. and Mathis, P. (1989) Photosynth. Res. 20, 279–289.
15 Chapman, D.J. and Barber, J. (1989) Physiol. Plant. 76, A14.
16 Van Mieghem, F., Nitschke, W., Mathis, P. and Rutherford, A.W. (1989) Physiol. Plant 76, A113.
17 Chapman, D.J., Gounaris, K. and Barber, J. (1988) Biochim. Biophys. Act 933, 423–431.
18 Gast, P. and Hoff, A.J. (1978) FEBS Lett. 85, 183–188.
19 Rutherford, A.W. (1986) Biochem. Soc. Trans. 14, 15–17.
20 Kleibeuker, J.F. and Schaafsma, T.J. (1974) Chem. Phys. Lett. 29, 116–122.
21 Hägele, W., Schmid, D. and Wolf, H.C. (1978) Z. Naturforsch. 33a, 83–93.
22 Ghanotakis, D.F., Babcock, G.T. and Yocum, C.F. (1984) Biochim. Biophys. Acta 765, 388–398.